the plant journal

SEB Society for Experimental Biology

The Plant Journal (2013) **73,** 640–652 doi: 10.1111/tpj.12063

The tomato *cis*–prenyltransferase gene family

Tariq A. Akhtar, Yuki Matsuba, Ines Schauvinhold, Geng Yu, Hazel A. Lees, Samuel E. Klein and Eran Pichersky*
Department of Molecular, Cellular and Developmental Biology, University of Michigan, Ann Arbor, MI 48109, USA

Received 15 August 2012; revised 25 October 2012; accepted 29 October 2012; published online 31 December 2012.
*For correspondence (e-mail lelx@umich.edu).

SUMMARY

***cis*–prenyltransferases (CPTs) are predicted to be involved in the synthesis of long-chain polyisoprenoids, all with five or more isoprene (C5) units. Recently, we identified a short-chain CPT, neryl diphosphate synthase (NDPS1), in tomato (*Solanum lycopersicum*). Here, we searched the tomato genome and identified and characterized its entire CPT gene family, which comprises seven members (*SlCPT1–7*, with *NDPS1* designated as *SlCPT1*). Six of the *SlCPT* genes encode proteins with N–terminal targeting sequences, which, when fused to GFP, mediated GFP transport to the plastids of Arabidopsis protoplasts. The SlCPT3–GFP fusion protein was localized to the cytosol. Enzymatic characterization of recombinant SlCPT proteins demonstrated that SlCPT6 produces *Z,Z*–FPP, and SlCPT2 catalyzes the formation of nerylneryl diphosphate while SlCPT4, SlCPT5 and SlCPT7 synthesize longer-chain products (C25–C55). Although no *in vitro* activity was demonstrated for SlCPT3, its expression in the *Saccharomyces cerevisiae* dolichol biosynthesis mutant (*rer2*) complemented the temperature-sensitive growth defect. Transcripts of *SlCPT2*, *SlCPT4*, *SlCPT5* and *SlCPT7* are present at low levels in multiple tissues, *SlCPT6* is exclusively expressed in red fruit and roots, and *SlCPT1*, *SlCPT3* and *SlCPT7* are highly expressed in trichomes. RNAi-mediated suppression of *NDPS1* led to a large decrease in β–phellandrene (which is produced from neryl diphosphate), with greater reductions achieved with the general 35S promoter compared to the trichome-specific MKS1 promoter. Phylogenetic analysis revealed CPT gene families in both eudicots and monocots, and showed that all the short-chain CPT genes from tomato (*SlCPT1*, *SlCPT2* and *SlCPT6*) are closely linked to terpene synthase gene clusters.**

Keywords: *cis*–prenyltransferase, polyisoprenoid, polyprenol, dolichol, monoterpene, *Solanum lycopersicum*.

INTRODUCTION

Plant isoprenoids represent a group of structurally diverse compounds that include photosynthetic pigments, sterols, hormones, redox co-factors in electron transport, and various specialized metabolites that are unique to particular plant lineages (Kirby and Keasling, 2009). These compounds are synthesized from common five-carbon (C5) isoprene building blocks that originate from two distinct pathways (McGarvey and Croteau, 1995; Rodríguez-Concepción and Boronat, 2002). The mevalonate (MVA) pathway in the cytosol produces isopentenyl diphosphate (IPP), while the methylerythritol phosphate (MEP) pathway in the plastids produces both IPP and its isomer, dimethylallyl diphosphate (DMAPP).

Isoprenoid synthesis is initiated by condensation of IPP with DMAPP. Successive head-to-tail additions of IPP generate longer-chain polyisoprenoids that typically range in size from C15 to C120. The sequential transfer of IPP units to allylic diphosphate acceptors is catalyzed by the class of enzymes known as prenyltransferases. Depending on the stereochemistry of the polyisoprenoid product, these enzymes are classified as either *trans*–prenyltransferases (TPTs) or *cis*–prenyltransferases (CPTs). Despite similarities in substrate preference and reaction products, TPTs and CPTs utilize different catalytic mechanisms and may be readily distinguished from one another by their primary amino acid sequences (Liang *et al.*, 2002; Kharel and Koyama, 2003).

Several plant TPTs involved in the synthesis of geranyl diphosphate (GPP, C10), *trans,trans*–farnesyl diphosphate (FPP, C15), all-*trans*–geranylgeranyl diphosphate (GGPP, C20) and solanesyl diphosphate (SPP, C45) have been identified and characterized (Burke *et al.*, 1999; Hirooka *et al.*, 2003; Lange and Ghassemian, 2003; Ducluzeau *et al.*, 2012). The products of these enzymes provide the precursors for brassinosteroids, carotenoids, gibberellins, prenylquinones, sterols and a variety of terpenes. Comparatively little is known about plant CPTs. On the other hand, the roles of bacterial, yeast and mammalian CPTs are well

established. In bacteria, CPTs synthesize long-chain polyisoprenoid diphosphates (C50–C55) that serve as lipid carriers in cell-wall peptidoglycan biosynthesis. In yeast and mammals, CPTs produce dehydrodolichyl diphosphate, the precursor of dolichol, a mixed *cis,trans*–polyisoprenoid (C75–C95) with a reduced double bond in the α isoprene unit that has an indispensible role in the post-translational modification of proteins (Figure 1).

Polyisoprenoids have been identified in numerous plants, and broadly fall into one of two classes: dolichols and polyprenols (Swiezewska and Danikiewicz, 2005; Skorupinska-Tudek *et al.*, 2008). As in animals, plant dehydrodolichyl diphosphates are synthesized by CPTs that elongate *trans*–FPP with C5 units in a *cis* orientation resulting in a final linear polymer that is typically 70–120 carbons in length. Polyprenyl diphosphates are structurally similar but are unsaturated at the terminal isoprene position (Figure 1). Moreover, polyprenols from plant sources appear to be initiated using *trans*–substrates of varying length. The so-called 'betulaprenols' and 'ficaprenols' are synthesized from *trans*–FPP and *trans*–GGPP, respectively.

Clear genomic evidence exists for the distribution of CPT-like proteins throughout the plant kingdom. For instance, in *Arabidopsis thaliana*, a CPT gene family with nine members has been reported (Surmacz and Swiezewska, 2011). One member of this group, ACPT/DPS (At2g23410), contributes toward the biosynthesis of long-chain polyisoprenoids (Cunillera *et al.*, 2000; Oh *et al.*, 2000), while another member, AtHEPS, was recently identified as a heptaprenyl diphosphate synthase (Kera *et al.*, 2012). However, functions have not been assigned for the remaining members of the Arabidopsis CPT family. Other reports of plant CPTs include several genes from *Hevea brasiliensis* and *Taraxacum brevicorniculatum* that are associated with synthesis of natural rubber particles, and the *LLA66* gene expressed in the anthers of *Lilium longiflorum* that appears to be involved in microspore development (Asawatreratanakul *et al.*, 2003; Schmidt *et al.*, 2010; Liu *et al.*, 2011; Post *et al.*, 2012). Finally, CPTs provide the precursors for monoterpene and sesquiterpene biosynthesis, respectively, in the glandular (type VI) trichomes of two *Solanum* species, cultivated tomato (*S. lycopersicum*) and its wild relative, *S. habrochaites*. In tomato, neryl diphosphate synthase 1 (NDPS1) condenses IPP and DMAPP to neryldiphosphate (NPP), and a monoterpene synthase, β–phellandrene synthase 1 (PHS1), uses NPP to produce β–phellandrene and several other monoterpenes (Schilmiller *et al.*, 2009). In *S. habrochaites*, a *cis,cis*–farnesyl diphosphate synthase (*z*FPS) catalyzes two sequential additions of IPP to DMAPP to produce *cis,cis*–farnesyl diphosphate (*Z,Z*–FPP), and a sesquiterpene synthase, santalene/bergamotene synthase (SBS), converts *Z,Z*–FPP to santalene and bergamotene (van Der Hoeven *et al.*, 2000; Sallaud *et al.*, 2009).

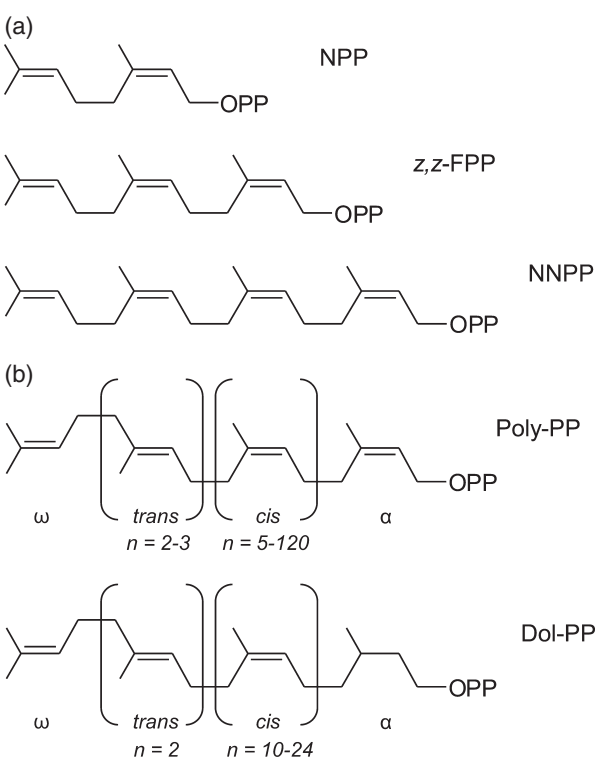

Figure 1. The structures of *cis*–prenyldiphosphates.
(a) The short-chain *cis*–prenyldiphosphates neryl diphosphate (NPP), *cis–cis* –farnesyl diphosphate (*Z,Z*–FPP) and nerylneryl diphosphate (NNPP, equivalent to *cis–cis–cis*–geranylgeranyl diphosphate).
(b) The long-chain *cis*–prenyldiphosphates polyprenyl diphosphate (Poly-PP) and dolichyl diphosphate (Dol-PP).

Although the function of the vast majority of plant CPT genes whose sequences are found in various databases is not well established, their homology to dehydrodolichyl diphosphate synthases from non-plant species suggests that they are involved in the synthesis of long-chain polyisoprenoid diphosphates. At present, NDPS1 and *z*FPS are the only CPTs from plants that are known to catalyze the formation of short-chain prenyl diphosphates ($\leq$C20). To understand the evolutionary origin of CPTs that synthesize short-chain prenyl diphosphates, we have analyzed the entire CPT gene family present in the genome of *S. lycopersicum*, taking advantage of the recently released tomato genome sequence.

RESULTS

Identification of the tomato CPT gene family

To identify all genes with homology to NDPS1, we searched the recently released tomato genome sequence (http://solgenomics.net). This search identified six additional *CPT*-like gene sequences encoding proteins with homology to NDPS1 (SlCPT1), which we named *SlCPT2–7* (Figure 2a and Figure S1). In cases where a gene sequence was incomplete, the regions spanning the gaps were amplified from genomic DNA to complete the sequence of

the gene. We also screened EST databases (http://solgenomics.net/), and found representatives of all seven genes, but no additional sequences. We conclude that the tomato CPT gene family contains seven members, including *NDPS1*. *SlCPT2* is located in the same cluster of terpene synthase genes on chromosome 8 as *NDPS1* (Falara *et al.*, 2011), *SlCPT3* is located on chromosome 3, *SlCPT4* and *SlCPT5* are tandemly linked (in the same direction) and are present on chromosome 10, and *SlCPT6* and *SlCPT7* are both located on chromosome 6 but 9.6 Mb apart, with *SlCPT6* embedded within a terpene synthase gene cluster (Falara *et al.*, 2011).

Based on sequence homology to *NDPS1* and related sequences from other species, it was predicted that *SlCPT2* contains three introns (same number and position as in *NDPS1*), *SlCPT3* contains no introns, and *SlCPT4–7* each contain two introns, in positions equivalent to introns 2 and 3 in *NDPS1* (Figure 2a and Figure S1). To verify the predicted exon/intron boundaries for each gene model (Figure 2a and Figure S1), we amplified full-length coding sequences for each gene by RT–PCR. Full-length cDNAs with all introns removed were obtained for all *SlCPT* genes. However, fully processed *SlCPT6* cDNAs were only obtained when using RNA prepared from root to red fruits; RT–PCR products obtained from all other source tissues revealed transcripts with an unspliced first intron (and therefore probably non-functional because of stop codons introduced in-frame).

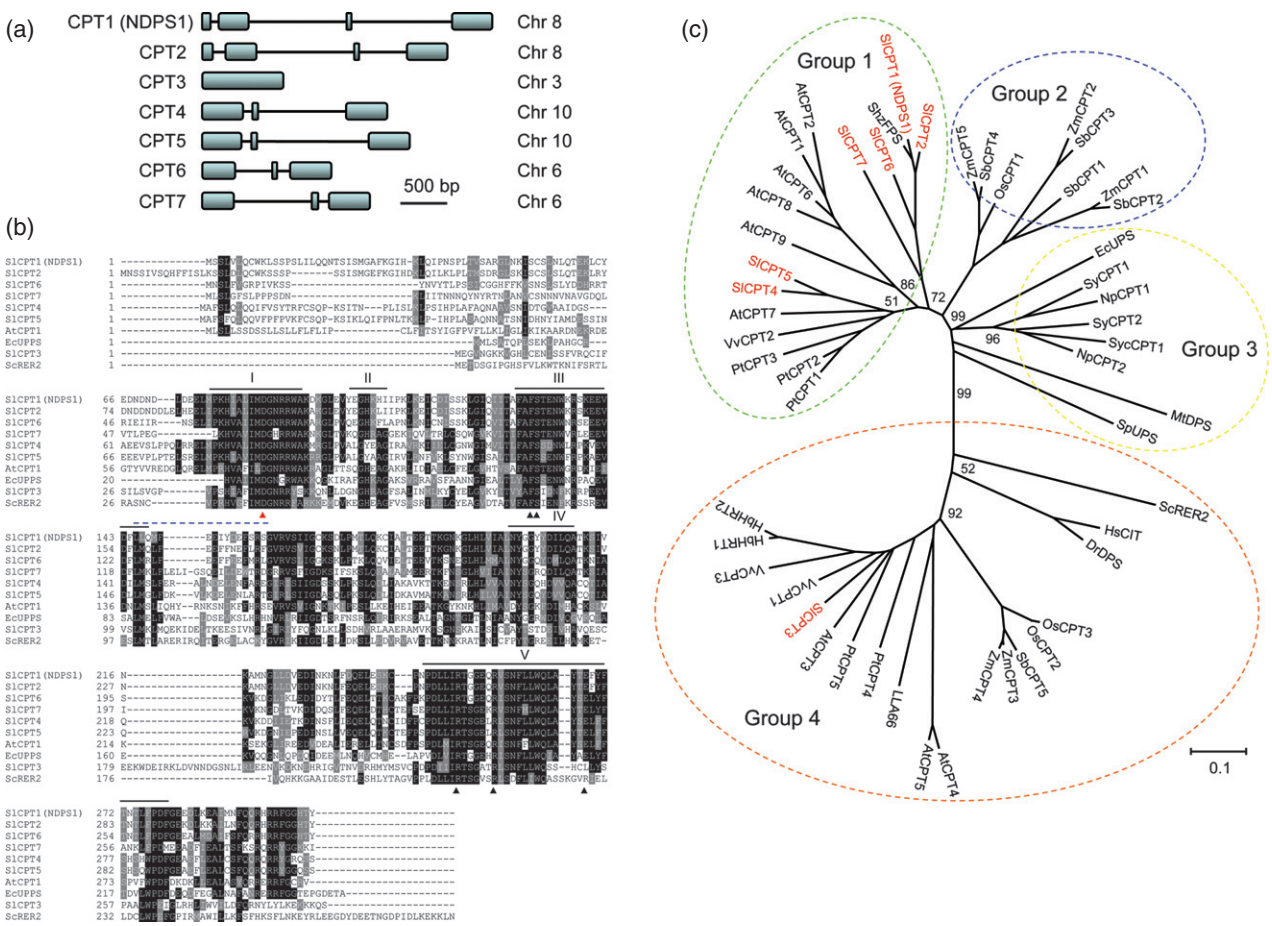

Figure 2. Identification of the tomato *CPT* gene family.

(a) Gene organization of *SlCPT1–7*. *SlCPT1*, *SlCPT2*, *SlCPT6* and *SlCPT7*, and *SlCPT4* and *SlCPT5* are located on chromosomes 8, 6 and 10, respectively, and *SlCPT3* is located on chromosome 3. The coding sequence for each gene was verified by PCR and RT–PCR.

(b) Amino acid sequence alignment of SlCPT1–7 with functionally characterized CPTs. The deduced amino acid sequences of SlCPT1–7 are compared to previously reported CPTs from *E. coli* (EcUPS), yeast (ScRER2) and Arabidopsis AtCPT1. Identical residues are highlighted in black and similar residues are highlighted in gray. Black horizontal lines indicate the five conserved regions (regions I–V) present in CPTs, and the dashed blue line indicates the region of CPT proteins that affects product chain length. The red triangle indicates the conserved Asp residue involved in catalysis, and black triangles indicate that are residues important for substrate recognition.

(c) Neighbor-joining phylogenetic tree of the tomato CPTs and predicted CPTs from six other plant species (see text), as well as representative CPT sequences from bacteria, yeast and animal species. Branch lengths represent the number of amino acid substitutions per position. Bootstrap values (1000 replicates) are indicated next to the branches, and values <50 are omitted for clarity. Sequence names and accession numbers are given in Figures S1 and S2.

Alignment of the tomato deduced protein sequences with previously characterized CPTs from *Escherichia coli*, *Saccharomyces cerevisiae* and *A. thaliana* revealed four general features (Figure 2b). First, the five characteristically conserved regions (regions I–V) of CPTs (Kharel and Koyama, 2003) are also conserved in the tomato CPT proteins, including the Asp residue in region I that critically affects catalysis. Second, the five residues implicated in substrate binding (F70, S71, R194, R200 and E213; amino acid numbers corresponding to the *E. coli* enzyme) are present in all SlCPTs, except for SlCPT3, which contains an L residue in place of E. Interestingly, in the yeast dehydrodolichyl diphosphate synthase, the residue at position 213 is not an E but an R. Third, the SlCPT3 protein is the only member of the tomato CPT family without an N–terminal extension, a feature that is shared with yeast and *E. coli* proteins. Lastly, the region inferred from crystallographic and mutagenesis studies to impact product chain length (indicated by the dashed blue line between regions III and IV in Figure 2b) varies significantly among SlCPTs. The presence of additional residues in this region is normally associated with long-chain elongating enzymes, such as the CPT from yeast. Only SlCPT3 has a full complement of amino acids in this region, while the other tomato proteins lack between one and seven residues in this stretch.

To explore the evolutionary relationships between the tomato CPT family and those found in other plants, an expanded search of six plant genomes [three dicots (*Arabidopsis thaliana*, *Vitis vinifera* and *Populus trichocarpa*) and three monocots (*Oryza sativa*, *Sorghum bicolor* and *Zea mays*)] was performed. A total of 30 additional CPT-like sequences from these six species (*AtCPT1–9*, *VvCPT1–3*, *PtCPT1–5*, *OsCPT1–3*, *SbCPT1–5* and *ZmCPT1–5*) were identified and used to construct an unrooted phylogenetic tree together with representative CPTs from animals, eubacteria and yeast (Figure 2c). This analysis placed CPTs into four phylogenetic groups, with group 1 and group 2 representing dicot- and monocot-specific branches, respectively. Six of the seven tomato CPT genes – *SlCPT1*, *SlCPT2*, *SlCPT4*, *SlCPT5*, *SlCPT6* and *SlCPT7* – are in group 1. The CPTs from cyanobacteria form a distinct clade, group 3, with other bacterial CPTs from the phyla of actinobacteria, proteobacteria and firmicutes. Group 4, in which *SlCPT3* is placed, includes CPTs known to synthesize dolichols in yeast, humans and zebrafish, the long-chain CPTs from *Hevea brasiliensis* involved in natural rubber biosynthesis, as well as one to three sequences found in the genomes of each of the six representative plant species. The majority of plant sequences in group 4 (with the exception of VvCPT1 and ZmCPT3) also appear to lack N–terminal extensions.

SlCPT gene expression

The widespread expression of the *SlCPT* genes is apparent from searches of the publically available tomato EST collections. To determine the relative amount and tissue distribution of the *SlCPT* transcripts, the expression of each *SlCPT* gene was measured in a selection of tomato tissues by real-time PCR. Expression was quantified by the standard curve method in order to compare absolute

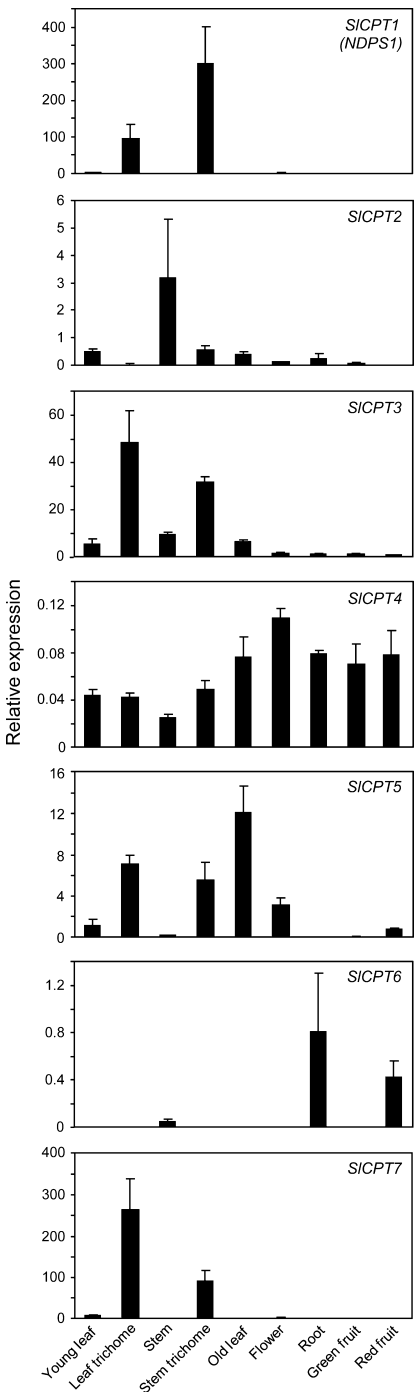

Figure 3. Expression of members of the *SlCPT* gene family in various plant organs and tissues. Expression values were fitted to standard curves for each gene and normalized to those for an elongation factor 1α (control). Values are means ±SD from 3 to 4 biological replicates.

expression levels between each gene (Figure 3). As previously reported, *NDPS1* was expressed predominantly in stem and leaf trichomes at very high levels (Schilmiller *et al.*, 2009), and a similar pattern of expression was observed for *SlCPT7*. Although transcripts for *SlCPT3* and *SlCPT5* were also found to be enriched in trichomes, expression was detected to varying levels in all other tissues examined. *SlCPT2* and *SlCPT4* were also expressed in all tissues, but at relatively low levels compared with other members of the family, while *SlCPT6* was expressed almost exclusively in roots and red fruits.

Subcellular localization of SlCPTs

The subcellular distributions predicted by various algorithms (TargetP (http://www.cbs.dtu.dk/services/TargetP/), WoLF PSORT (http://wolfpsort.org/) and Predator (http://urgi.versailles.inra.fr/predotar/predotar.html)) were inconclusive in determining whether the N–terminal extensions present on each *SlCPT* gene (with the exception of *SlCPT3*) encoded a *bona fide* transit peptide. Therefore, the first approximately 120 amino acids of each *SlCPT* gene were fused to GFP and transiently expressed in Arabidopsis mesophyll protoplasts to determine whether these N–terminal extensions mediate transport of GFP to distinct subcellular locations. For *SlCPT3*, which lacks an obvious targeting peptide, the entire coding region was fused to GFP. Consistent with the absence of a targeting sequence, SlCPT3 appeared to be localized to the non-organellar area of the cell, presumably the cytosol (Figure 4). All other members of the CPT family were found to be associated with plastids, with two distinct patterns of GFP fluorescence observed. For *SlCPT1*, *2* and *5*, a uniform GFP fluorescence signal was observed evenly throughout the plastids. On the other hand, a punctate pattern of GFP fluorescence was observed for *SlCPT4*, *6* and *7* that coincided with chlorophyll autofluorescence (Figure 4). To rule out the possibility that these proteins localize to the mitochondria, the experiments were performed in transgenic protoplasts constitutively expressing a mitochondrial-localized CFP reporter. The punctate GFP fluorescence in these experiments did not coincide with the mitochondrial CFP signal (see Figure 4 for results with *SlCPT6* and *SlCPT7*).

Enzymatic characterization of SlCPTs

To date, all plant CPTs that have been enzymatically characterized are involved in either dolichol biosynthesis (>C75) or synthesis of the short-chain prenyl diphosphates NPP and *Z,Z*–FPP (Figure 1). However, CPTs associated with the production of medium-chain polyisoprenoids (C25–C75) have yet to be identified, despite the reported occurrence of these compounds as well as the enzymatic activities responsible for their synthesis in plants. To examine the enzymatic properties of each SlCPT, the cDNAs for each gene were expressed in *E. coli* to give truncated proteins (without transit peptide) with C–terminal His tags, as previously done for NDPS1 (Schilmiller *et al.*, 2009). SlCPT3, which lacks a transit peptide, was produced as the full-length protein. The recombinant proteins were purified by Ni^{2+} affinity chromatography and assayed for CPT activity using ^{14}C–IPP and a variety of available initiator substrates, including DMAPP, GPP, NPP, all-*cis*– and all-*trans*–FPP, and all-*trans*–GGPP. Products were analyzed by radio-TLC (and, in the case of SlCPT2 and SlCPT6, also by

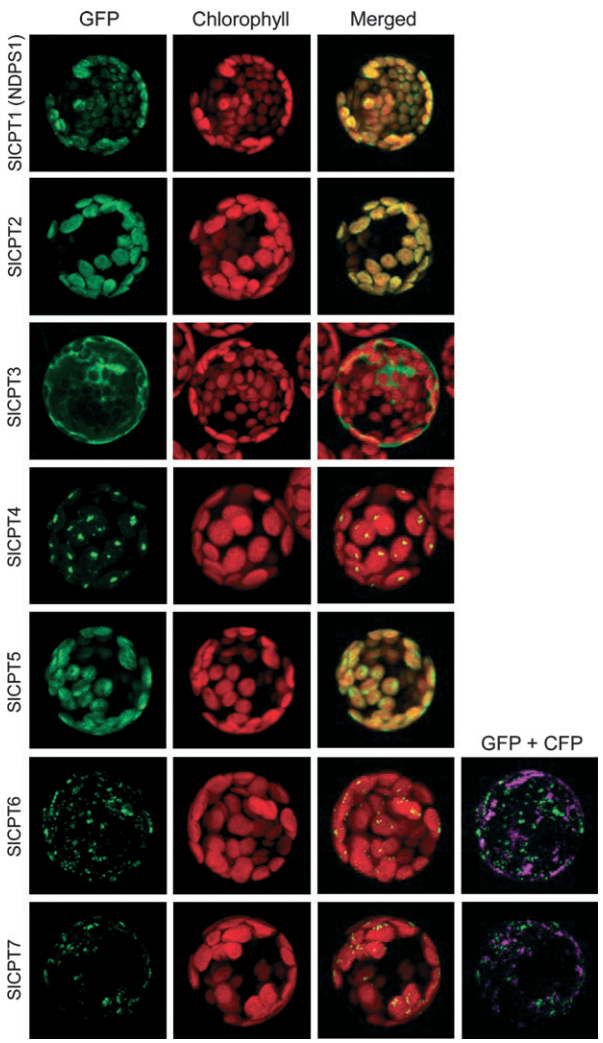

Figure 4. Subcellular localization of SlCPTs.
Determination of subcellular localization was performed in Arabidopsis mesophyll protoplasts analyzed by confocal laser scanning microscopy. For *SlCPT1*, *2*, *4*, *5*, *6* and *7*, the first approximately 120 amino acids for each gene was fused to downstream GFP. For *SlCPT3*, which lacks an obvious targeting peptide, the entire coding region was fused to GFP as a C–terminal fusion. The column labeled 'GFP' shows the location of each fusion protein, as indicated on the left. The column labeled 'Chlorophyll' indicates the autofluorescence (red) associated with the location of plastids, and the column labeled 'Merged' represent the two combined fluorescent images. For SlCPT6 and SlCPT7, the assays were performed in protoplasts expressing an endogenous CFP reporter. The column labeled GFP + CFP indicates combined fluorescence of the GFP signal and the endogenous mitochondrial-localized CFP (pseudocolored in magenta).

Table 1 Enzyme properties of recombinant SlCPTs

Enzyme	Amino acids	Preferred substrate	Product	Product size
SlCPT1	303	DMAPP	NPP	C10
SlCPT2	314	DMAPP[a]	*NNPP*	C20
SlCPT3	290	*trans*–FPP	Polyprenyl-PP	C65
SlCPT4	308	NPP, GPP[b]	Polyprenyl-PP	C55
SlCPT5	313	*trans*–FPP, *Z,Z*–FPP[c]	Polyprenyl-PP	C60
SlCPT6	285	NPP	*Z,Z*–FPP	C15
SlCPT7	287	GGPP	Polyprenyl-PP	C35

[a]NPP and *Z,Z*–FPP, [b]*trans*–FPP and *Z,Z*–FPP, and [c]NPP were utilized with slightly lower efficiency.

GC–MS). The tested tomato CPTs (with the exception of SlCPT3) were broadly characterized as either short-chain CPTs (SlCPT2 and SlCPT6) or medium-chain CPTs (SlCPT4, SlCPT5 and SlCPT7). The range of substrates used by these enzymes is summarized in Table 1, and the products produced from the substrate for which the highest activity was observed are shown in Figure 5(a). SlCPT6's preferred acceptor substrate was NPP, and the product obtained in this reaction was *Z,Z*–FPP (Figure 5a and Figure S3). SlCPT2 preferred DMAPP, and produced a product tentatively identified as nerylneryl diphosphate (NNPP, equivalent to *Z,Z,Z*–GGPP) (Figure S4), SlCPT4 and SlCPT5 produced polyprenyl diphosphates with a range of C5 subunits but with the predominant products being C50–55 and C55–65, respectively (Figure 5a). Both of these enzymes were able to elongate all substrates that were assayed, but SlCPT4 preferred NPP and GPP while SlCPT5 utilized *trans*–FPP and *Z,Z*–FPP most efficiently (Table 1). SlCPT7 was the only member to produce 'ficaprenols', as it uses GGPP exclusively and gives a range of polyprenols, with C25–C35 products being dominant (Figure 5a).

No *in vitro* activity with any substrate was demonstrated for *E. coli*-produced SlCPT3. As SlCPT3 is most closely related to dehydrodolichyl diphosphate synthases from eukaryotes (Figure 2c), and no other member of the SlCPT family appears to produce the long-chain (C75–C90) products that are typical of plant dolichols, we tested whether SlCPT3 complimented the growth defect of the *Saccharomyces cerevisiae* dolichol biosynthesis mutant, *rer2*, which has a severely retarded growth rate at temperatures above 30°C (Sato *et al.*, 1999) as a positive control, the *E. coli* undecaprenyl pyrophosphate synthase (UPPS) that compliments the rer2 growth defect (Rush *et al.*, 2010), was also introduced into the mutant cells. When *SlCPT3* was introduced into *rer2* mutant cells (*rer2*Δ/SlCPT3), the temperature-sensitive growth defect was rescued, as cells readily grew at 33°C whereas mutant yeast cells did not (Figure 5b). The restoration of growth was associated with significantly higher total CPT enzyme activity on microsomal membranes (the site of dolichol biosynthesis) from cells of *rer2*Δ/SlCPT3 compared to the *rer2* mutant (Figure 5c). The enzymatic products of these CPT assays were resolved by radio-TLC and shown to include a long-chain polyprenyl diphosphate (C65) that was synthesized by *rer2*Δ/SlCPT3 microsomes but not by microsomes from the *rer2* mutant (Figure 5d).

Constitutive and trichome-specific RNAi-mediated knockdown of *NDPS1*

NDPS1 catalyzes the formation of NPP, which is used as a substrate by PHS1 to produce β–phellandrene and several other monoterpenes (Schilmiller *et al.*, 2009). *NDPS1* is expressed several hundred times more highly in type VI trichomes than in the rest of the plant (Figure 3) (Schilmiller *et al.*, 2009), and its contribution to monterpene synthesis (mostly β–phellandrene) in these trichomes has been identified previously (Schilmiller *et al.*, 2009). However, the trichomes constitute only a very small part of the mass of the cultivated tomato plant. To determine whether the low-level expression of *NDPS1* in non-trichome tissue contributes to monoterpene biosynthesis in tomato, we performed RNAi-mediated knockdown of NDPS1 using two independent RNAi constructs, one driven by the promoter of methylketone synthase 1 (*MKS1*), a 3–ketoacid decarboxylase gene that is highly expressed in type VI trichomes (Figure 6a) (Fridman *et al.*, 2005), and one driven by the CaMV 35S promoter.

We generated >40 transgenic tomato lines carrying Pro^{MKS}::$NDPS1^{RNAi}$ and Pro^{35S}::$NDPS1^{RNAi}$ constructs. From these lines, we identified those in which NDPS1 expression is most highly suppressed by performing solid-phase microextraction (SPME) on leaf volatiles and examining the β–phellandrene/β–caryophyllene ratio, as β–caryophyllene, a sesquiterpene, is a prominent tomato leaf volatile and is synthesized from the substrate *trans–trans*–FPP (Schilmiller *et al.*, 2010), and therefore its synthesis is not affected by suppressing NDPS1 transcript levels (Figure S4). For selected lines showing the greatest reduction in the β–phellandrene/β–caryophyllene ratio, a comparison of *NDPS1* transcript levels in total RNA extracted from whole leaves with that of control plants indicated a mean knockdown of 75 and 87% with the MKS1 and 35S promoters, respectively (Figure 6b). For RNA isolated from leaf trichomes of these transgenic lines, 76% *NDPS1* knockdown was observed in

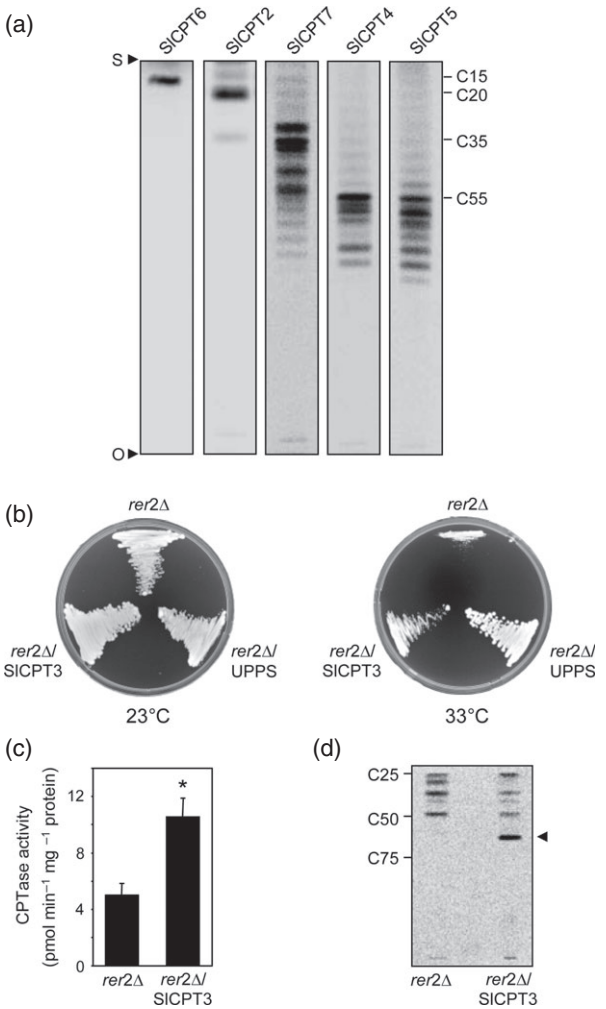

Figure 5. Enzymatic characterization of recombinant SlCPTs.
(a) Radio-TLC separation and analysis of the reaction products obtained from assays performed using SlCPT2, SlCPT4, SlCPT5, SlCPT6 and SlCPT7. Prior to analysis, the radiolabeled enzymatic products were dephosphorylated with alkaline phosphatase (for short-chain enzymatic products, <C25) or with acid (for longer-chain products), and then extracted using ethyl acetate (see Experimental procedures). Products were resolved on reversed-phase silica gel 60 Å plates using an acetone/water (39:1) solvent system and developed by phosphorimager analysis. The size of the major reaction product(s) were determined based on the migration of authentic polyprenol standards of known size (C10–C120) visualized by iodine vapor staining. The origin (O) and solvent front (S) are indicated on the left.
(b) Functional complementation of the yeast *rer2* mutant. Yeast *rer2* mutant cells were transformed with either *SlCPT3* or the *E. coli* UPPS gene (which had previously been shown to complement *rer2*, Rush *et al.*, 2010) under the transcriptional control of the native RER2 promoter. Transformed cells were grown on YPD plates and incubated at 23 and 33°C.
(c) Microsomal CPT activity from *rer2*Δ and *rer2*Δ/SlCPT3. Values are means ± SE from four independent microsomal membrane preparations, and the asterisk indicates a significant difference ($P < 0.05$).
(d) Radio-TLC separation of the reactions products obtained from CPT assays using microsomal membranes from *rer2*Δ and *rer2*Δ/SlCPT3. Note the presence of the C65 product (arrowhead) in *rer2*Δ/SlCPT3 microsomes.

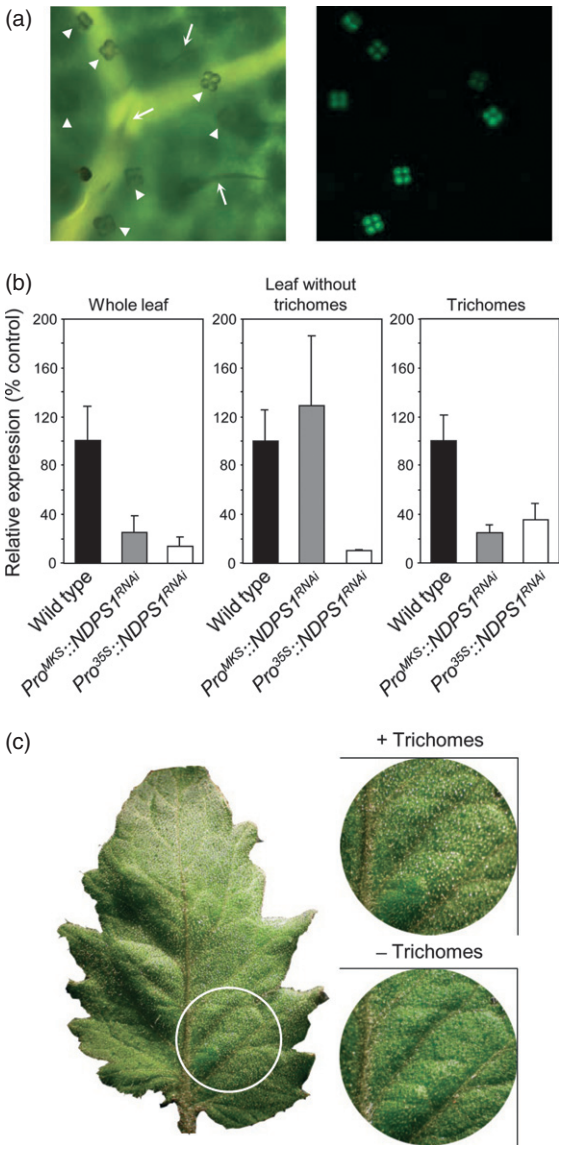

Figure 6. RNAi-mediated knockdown of *SlCPT1*.
(a) Bright-field (left) and GFP fluorescent (right) images of a tomato leaf stably expressing the MKS1–GFP reporter. The presence of the MKS1 promoter upstream of GFP guides expression exclusively to the head cells of type VI trichomes (indicated by arrowheads). Type I trichomes are indicated by arrows.
(b) *SlCPT1* knockdown in RNAi lines driven by the MKS1 ($Pro^{MKS}::CPT1^{RNAi}$) and 35S promoters ($Pro^{35S}::CPT1^{RNAi}$). *SlCPT1* expression was quantified by quantitative PCR, and values are mean expression levels ± SD from three biological replicates, expressed relative to that measured in wild-type tissue. For each RNAi construct, a minimum of three independent transgenic plants were sampled.
(c) Illustration of a tomato leaf with and without type VI trichomes. For trichome removal, a fully expanded young leaf was excised from the plant, placed under a dissecting microscope, and trichomes were removed by gently rolling a cotton swab across the leaf surface.

the $Pro^{MKS}::NDPS1^{RNAi}$ lines, while only 65% *NDPS1* knockdown was measured in $Pro^{35S}::NDPS1^{RNAi}$ lines (Figure 6b). On the other hand, for RNA isolated from leaves from which the glandular trichomes had been removed (Figure 6b,c), there was no reduction in NDPS1 transcript levels compared to control in the $Pro^{MKS}::NDPS1^{RNAi}$ lines, but a 90%

decline in NDPS1 transcript abundance was observed in the *Pro*^{35S}*::NDPS1*^{RNAi} lines. Taken together, these results indicate that, while *NDPS1* is predominantly expressed in glandular trichomes, it is also expressed elsewhere in the leaf, and that NDPS1 transcript reduction in non-trichome cells is achieved in *Pro*^{35S}*::NDPS1*^{RNAi} but not *Pro*^{MKS}*:: NDPS1*^{RNAi} lines. However, the latter construct was somewhat better at suppressing *NDPS1* gene expression in the trichomes (Figure 5b, right).

To examine the effect on β–phellandrene synthesis of reduction in *NDPS1* transcript levels by the two RNAi constructs, total volatile compounds were extracted from leaves of plants showing high levels of *NDPS1* transcript reduction. The amounts of β–phellandrene and β–caryophyllene were quantified and compared to those found in wild-type leaf tissue. On average, the *Pro*^{MKS}*::NDPS1*^{RNAi} lines exhibited a 56% decrease in extractable β–phellandrene, while a decrease of more than 92% was observed in *Pro*^{35S}*:: NDPS1*^{RNAi} lines (Figure 7). There was no significant difference in the amount of β–caryophyllene between wild-type and either RNAi line, or in the total sesquiterpene content (Figure 7). When trichomes were removed from wild-type leaves, extractable β–phellandrene and β–caryophyllene levels fell by 72 and 89%, respectively, indicating that the majority of each of these compounds, but not all, is found in the trichome, as previously observed (Schilmiller *et al.*, 2009). Consistent with this result, when β–phellandrene levels were compared in plants from which trichomes had been removed, these levels were the same for trichome-less wild type leaves and the *Pro*^{MKS}*::NDPS1*^{RNAi} line, but the *Pro*^{35S}*:: NDPS1*^{RNAi} line showed an 84% reduction in extractable β–phellandrene levels compared with trichome-less wild-type leaves, with no significant changes in β–caryophyllene. Taken together, these results indicate that a small but significant proportion of β–phellandrene is found outside the glandular trichomes, and that impaired NPP synthesis significantly affects the amount of β–phellandrene synthesis throughout the leaf tissue.

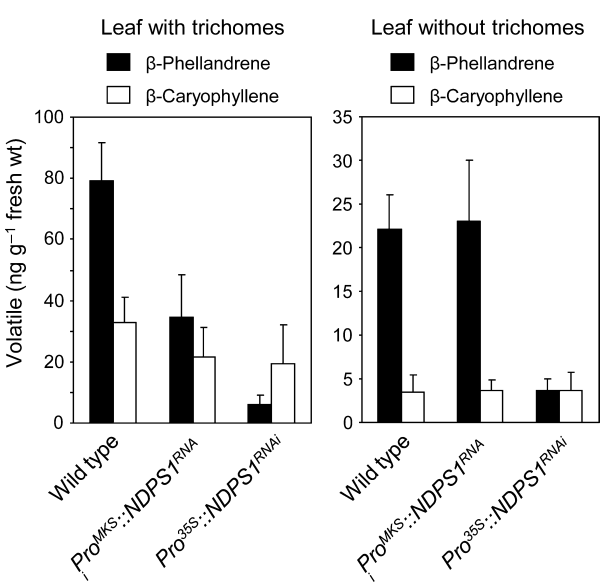

Figure 7. Impact of SlCPT1 knockdown on tomato leaf terpenes. Total extractable β–phellandrene and β–caryophyllene levels from *Pro*^{MKS}*::CPT1*^{RNAi} and *Pro*^{35S}*::CPT1*^{RNAi} RNAi lines compared to wild-type. Terpenes were extracted by grinding leaf tissue, with or without trichomes, in hexane. Extracts were analyzed by GC–MS (see Experimental procedures). For each RNAi construct, a minimum of three independent transgenic plants were sampled.

DISCUSSION

The tomato CPT family contains seven members, six of which encode plastidic proteins

To date, complete bioinformatics analysis of a plant CPT family has only been reported for Arabidopsis (Surmacz and Swiezewska, 2011). However, of the nine Arabidopsis CPT genes identified, the function of only one gene (*AtCPT1*) has been described (Cunillera *et al.*, 2000; Oh *et al.*, 2000). This gene was demonstrated to partially rescue the yeast dehydrodolichyl diphosphate synthase mutant, *rer2*, and was therefore deduced to encode the Arabidopsis equivalent. The subcellular localizations of the Arabidopsis proteins have also not been reported. Here we show that tomato has seven CPT genes, one of which, *SlCPT3*, is closely related to dehydrodolichyl diphosphate synthases from eukaryotes (group 4, three genes in Arabidopsis), with the other six tomato CPT genes residing in a group comprised of dicot-specific CPTs (group 1; six genes in Arabidopsis, including *AtCPT1*; Figure 1). Examination of the phylogenetic tree shown in Figure 1 indicates that a recent series of gene duplications occurred in both tomato and Arabidopsis after the split of the two lineages, with *SlCPT4* and *SlCPT5* being one example of genes related to each other by such a duplication, and *SlCPT1*, *SlCPT2*, *SlCPT6* and *SlCPT7* being a second example in tomato, while *AtCPT1*, *AtCPT2*, *AtCPT6*, *AtCPT8* and *AtCPT*9 were created by duplications in Arabidopsis after the split of the tomato and Arabidopsis lineages from each other.

Bioinformatic analysis and subcellular localization experiments indicate that SlCPT3 does not have an N–terminal extension and appears to reside in the cytosol, while the other six tomato CPT proteins contain a transit peptide at their N–terminus and are localized to the plastids (Figures 1 and 3). The observation that most tomato *cis*–prenyltransferases reside in the plastids fits well with previous reports indicating that the bulk of polyisoprenoid biosynthesis occurs in this compartment (Spurgeon *et al.*, 1984; Sakaihara *et al.*, 2000; Skorupinska-Tudek *et al.*, 2008), a compartment that also contains an active MEP pathway that leads to the synthesis of IPP, DMAPP, GPP, all-*trans*–FPP and GGPP (McGarvey and Croteau, 1995; Bonk *et al.*, 1997; Sanmiya *et al.*, 1999; Phillips *et al.*,

2008), and also NPP and *Z,Z*–FPP, at least in *Solanum* (Sallaud *et al.*, 2009; Schilmiller *et al.*, 2009).

SlCPT4, SlCPT5 and SlCPT7 produce medium-length chain polyisoprenyl diphosphates

A significant proportion of the polyisoprenoids that are found in plant tissues are of medium chain length (C25–C65); however, no CPTs responsible for their synthesis have been identified (Swiezewska and Danikiewicz, 2005). We show here that SlCPT4, 5 and 7 synthesize polyprenols in that range. SlCPT4 is expressed relatively uniformly in all tissues, albeit at a much lower level than either SlCPT5 or SlCPT7 (Figure 2). It is noteworthy that SlCPT4 appears to prefer GPP and NPP as substrates, given that all plant polyisoprenoids that have been identified so far contain either two (ω–*trans*$_2$–*cis*$_n$) or three (ω–*trans*$_3$–*cis*$_n$) *trans* isoprene units located at the ω–terminus of the molecule (Skorupinska-Tudek *et al.*, 2008). In the case of SlCPT4, elongation of a C10 substrate (such as GPP or NPP) results in a mono-*trans* type (ω–trans$_1$–*cis*$_n$), which has only been reported in bacteria (Schulbach *et al.*, 2000). On the other hand, SlCPT7 is the only tomato CPT member that strictly uses GGPP as the substrate, to give C25–35 products, thus appearing to be the only CPT in the tomato genome that synthesizes ficaprenols (ω–*trans*$_3$–*cis*$_n$), which have been identified in many other plants (Swiezewska *et al.*, 1994).

Despite the widespread occurrence of medium-chain products (C25–C65) such as those synthesized by SlCPT4, 5 and 7, their functional significance remains unclear. Medium- and long-chain polyisoprenoids are known to accumulate in senescing photosynthetic tissues, and their synthesis is stimulated by light (Chojnacki and Vogtman, 1984; Bajda *et al.*, 2005). Indirect evidence for the association of polyisoprenoids with plant cell walls comes from a recently characterized group of saprophytic bacteria that possess a unique polyisoprenoid-binding protein that aids in the dismantling of plant cell-wall material (Vincent *et al.*, 2010). It has been shown *in vitro* that polyisoprenoids alter the permeability of cellular membranes by increasing membrane fluidity (Vigo *et al.*, 1984; Ciepichal *et al.*, 2011). Also, the association of polyisoprenoids with specific membrane proteins is thought to influence translocation processes (Zhou and Troy, 2003). The incorporation of medium-chain lipophilic polyisoprenoids into membranes is plausible given the thickness of biological membranes (40–60 Å), although most plant polyisoprenoids are considerably shorter in length and only penetrate to the mid-bilayer region from one side of the membrane, much like the orientation of dolichol on the ER membrane (Schenk *et al.*, 2001; Zhou and Troy, 2003; Swiezewska and Danikiewicz, 2005). It is possible that plastid-derived polyisoprenoids associate with plastoglobuli (Austin *et al.*, 2006), the lipid-rich structures in plastids that also contain proteins involved in isoprenoid metabolism such as GGPP synthase (Cheniclet *et al.*, 1992; Ytterberg *et al.*, 2006). Intriguingly, proteins localized to this area of the plastid exhibit a punctate GFP fluorescence pattern within the chloroplast (Eugeni-Piller *et al.*, 2011), very similar to the pattern observed for SlCPT4, 6 and 7 in this study. The finding that all-*trans*–GGPP is the substrate for SlCPT7 further supports such an arrangement.

SlCPT3 is involved in dolichol biosynthesis

Phylogenetic analysis places SlCPT3 in a distinct group of CPTs (group 4) that include dolichol synthases from animals to yeast. When *SlCPT3* was expressed in the yeast dolichol biosynthesis *rer2* mutant, growth was restored and isolated microsomoal fractions synthesized a C65 isoprenyl diphosphate, further supporting the identification of SlCPT3 as a dehydrodolichyl diphosphate synthase. The localization of SlCPT3 to the cytosol, the site of dolichol biosynthesis on the ER membrane, is also consistent with this functional assignment.

The CPTs that synthesize dolichols in animals and yeast do not appear to function autonomously, but may require a partner protein known as NgBR (NUS1 in yeast) that also has a short CPT domain and another domain that is anchored to the ER membrane (Harrison *et al.*, 2011). The association between the CPT and this ER-anchored protein has been suggested to form the functional dolichol synthase (Schenk *et al.*, 2001; Harrison *et al.*, 2011). Indeed RNAi-mediated knockdown of NgBR results in defective N–linked protein glycosylation and dolichol synthesis in animals, while knockout mutants of the yeast and plant orthologs are lethal (Yu *et al.*, 2006; Zhang *et al.*, 2008; Harrison *et al.*, 2011). The fact that dehydrodolichyl diphosphate biosynthesis by a single eukaryotic protein has not been demonstrated *in vitro*, and that such an activity has only been recovered from microsomal membranes from animals, plants and yeast (Sakaihara *et al.*, 2000; Shridas *et al.*, 2003; Rush *et al.*, 2010), suggests that eukaryotic dehydrodolichyl diphosphate synthases are evolutionarily conserved. The observation that *rer2* yeast mutant cells complemented with *SlCPT3* synthesized an isoprenyldiphosphate of only 65 carbons suggests that the SlCPT3 protein may not work as well with NUS1 as the endogenous RER2 protein does.

Function and evolution of SlCPT1, SlCPT2 and SlCPT6, the short-chain *cis*–prenyldiphosphate synthases

Until recently, only short prenyl diphosphates (C_{10}, C_{15} and C_{20}) produced by *trans*–prenyl diphosphate synthases were known in plants. These *trans*–prenyl diphosphates (GPP, *trans*–FPP and all-*trans*–GGPP) are used to create volatile and non-volatile terpenes by mono-, sesqui- and diterpene synthases, respectively, to create sterols and carotenoids by head-to-head condensation of *trans*–FPP and all-*trans*-GGPP, respectively, and to prenylate other

molecules such as proteins and flavonols. In addition, they served as starter molecules for *cis*–prenyltransferases. The discovery of the synthesis of NPP and *Z,Z*–FPP by NDPS1 (SlCPT1) and *z*FPS in the trichomes of *S. lycopersicum* and *S. habroachaites* as the substrates of monoterpene and sesquiterpene synthases, respectively (Sallaud *et al.*, 2009; Schilmiller *et al.*, 2009) indicated additional biochemical functions for *cis*–prenyltransferases in plants.

Here we show that, in addition to NDPS1 (SlCPT1), tomato has two other CPTs that create short *cis*–prenyl diphosphates. SlCPT6's preferred acceptor substrate is NPP, and its product is *Z,Z*–FPP, a *cis*–prenyl diphosphate that has already been reported to be synthesized in another *Solanum* species (Sallaud *et al.*, 2009). SlCPT2 utilizes DMAPP as the acceptor molecule, and adds three IPP molecules to make NNPP, a compound (Figure 2) that has not previously been reported in plants. As previously reported (Falara *et al.*, 2011), *SlCPT1* and *SlCPT2* are embedded in a cluster of terpene synthase genes on chromosome 8, one of which (PHS1) uses the product of SlCPT1 (NPP) to produce β–phellandrene, the major monoterpene found in tomato trichomes (Schilmiller *et al.*, 2009). Here we show, via comparisons between NDPS1 RNAi lines driven by trichome-specific and CaMV 35S promoters, that *NDPS1* is expressed in non-trichome cells of the leaves as well, and contributes to monoterpene production there. On chromosome 6, a suite of terpene synthase genes also surround *SlCPT6* (Falara *et al.*, 2011). It is not uncommon to find clusters of non-homologous but functionally related genes in plants (Osbourn 2010), and it is likely that certain terpene synthases may have co-evolved with the short-chain CPTs.

These three short-chain SlCPTs from tomato are closely related to each other and to *z*FPS from *S. habrochaites* (Figure 2). Together they form a distinct sub-clade within the dicot-specific CPT group 1 that is most closely related to SlCPT7, the ficaprenol synthase. The phylogenetic analysis shows that the short-chain CPTs evolved by gene duplications that occurred after the split between the tomato and Arabidopsis lineages. It further shows that the progenitor of the short-chain tomato CPTs is a ficaprenol synthase, because this enzymatic activity is widespread in plants (Swiezewska and Danikiewicz, 2005) and therefore likely to be the ancestral function in this sub-clade.

Apart from the *Solanum* short-chain CPTs, such synthases have been identified only from bacteria (Schulbach *et al.*, 2000; Ambo *et al.*, 2008). Given that most CPTs of animal, bacteria and plant origin synthesize long-chain products, the identification of short-chain CPTs has stimulated interest in the structural basis for this activity (Kharel and Koyama, 2003). Based on the crystal structure of the long-chain CPT from *Micrococcus luteus* (UPPS), a large hydrophobic cleft near region III of this protein is believed to accommodate the enzymatic product during prenyl chain elongation (Fujihashi *et al.*, 2001). Kharel *et al.* (2006) noted a conspicuous reduction in the number of residues in this particular region of *z*FPP synthase from *Mycobacterium tuberculosis*, and insertion of only three residues into this region increased the product chain length from C15 to C70. Strikingly, the corresponding regions of SlCPT1, 2 and 6 are also lacking these residues, suggesting that this domain of CPT proteins critically affects chain length determination. It is noteworthy that SlCPT3, 4, 5 and 7, which synthesize longer chain products, all have more residues in this region (Figure 2b).

EXPERIMENTAL PROCEDURES

Chemicals and reagents

Authentic polyprenol standards were obtained from Indofine Chemical Company (http://www.indofinechemical.com/) (heptaprenol, C35) and Avanti Polar Lipids (http://avantilipids.com/) (polyprenol mixture, C65–C105). Substrates for CPT assays, including IPP, GPP, NPP, *trans*–FPP, Z,Z–FPP and all-*trans*–GGPP were obtained from Echelon Biosciences (http://www.echelon-inc.com/). Radiolabeled ^{14}C–IPP, 40–60 mCi (1.48–2.22 GBq mmol^{-1}; 0.02 mCi ml^{-1}) was obtained from PerkinElmer (http://www.perkinelmer.com/). TLC plates (silica gel 60, 20 cm × 20 cm) were obtained from Whatman (http://www.whatman.com/). Solid-phase microextraction (SPME) fibers and chromatography supplies were obtained from Supelco (http://www.sigmaaldrich.com/). All other chemicals were obtained from Sigma (http://www.sigmaaldrich.com).

Plant material and growth conditions

Arabidopsis thaliana (Col–0 ecotype) and tomato (cv. MP–1) plants (wild-type and transgenic) were grown in potting soil supplemented with Osmocote® (http://www.scotts.com/) in a growth chamber maintained at 22°C under a 12 h photoperiod (approximately 200 μmol m^{-2} sec^{-1} fluence rate generated by mixed cool-white fluorescent and incandescent bulbs). Red ripe tomato fruit was defined as breaker stage plus 7 days. Tomato stem and leaf trichomes were isolated by vigorously vortexing approximately 10 g of frozen plant material in a 50 ml centrifuge tube, and trichomes were collected from the bottom of the tube. Type VI tomato leaf trichomes were removed from 3-week-old tomato leaves by gently rolling a cotton swab over the leaf surface. The *Arabidopsis thaliana* line expressing a mitochondrial-localized CFP marker (Nelson *et al.*, 2007) was obtained from the Arabidopsis Biological Resource Center (stock number CS16262).

cDNA isolation and phylogenetic analysis of CPT sequences

Primers for cDNA isolation were designed based on the predicted open reading frame of each gene, and used to amplify the full-length cDNA by RT–PCR. All primers used in this study are listed in Table S1. RNA was extracted from various tomato tissues using and EZNA plant RNA mini kit (Omega Biotek) (http://www.omegabiotek.com/), reverse-transcribed using Superscript II reverse transcriptase (Invitrogen) (http://www.invitrogen.com/), and used directly for PCR amplification with KOD hot start DNA polymerase (Novagen) (http://www.emdmillipore.com/). PCR products were cloned into pGEM-T-Easy (Promega) (http://www.promega.com/) and their sequences were verified. Using the SlCPTs, all CPT-like sequences

in six additional plant genomes were identified (http://www.phytozome.net), and phylogenetic analysis of these sequences was performed using MEGA version 4 (Tamura *et al.*, 2007).

Gene expression

To quantify the mRNA abundance of each *SlCPT*, quantitative RT–PCR was performed as previously described (Schilmiller *et al.*, 2009).

Subcellular localization

The open reading frame of *SlCPT3* and a region corresponding to the first approximately 120 amino acids of the remaining *SlCPT* gene products were amplified, digested accordingly, and ligated into pSAT6A (Yu *et al.*, 2010), creating an in-frame C–terminal fusion protein with GFP. The constructs were mobilized into Arabidopsis protoplasts according to the 'tape sandwich' method (Wu *et al.*, 2009), and GFP fluorescence was visualized 16 h after transfection using a Leica SP5 laser scanning confocal microscope (http://www.leica-microsystems.com/) as previously described (Falara *et al.*, 2011). Spectral detection of CFP fluorescence was performed between 465 and 495 nm using a double dichroic 458/514 beam splitter.

Expression and purification of recombinant SlCPTs

Tomato CPTs were expressed and purified from *E. coli* cells as described previously (Schilmiller *et al.*, 2009).

CPT assays

cis–prenyltransferases activity assays were performed as described previously (Schilmiller *et al.*, 2009), and contained approximately 1–3 μg purified recombinant protein and 20 μM acceptor substrate, and were initiated by adding ^{14}C–IPP (50 μCi mmol^{-1}) at a final concentration of 80 μM (200 nCi), and incubated at room temperature for 30 min. To identify the products, 1 volume of 1 M HCl was added to the reaction mixture, and the hydrolyzed products were extracted with ethyl acetate and quantified by scintillation counting. Product analysis was also performed by thin-layer chromatography on reverse-phase 60 Å silica plates (Whatman), which were developed in acetone/water (39:1) and visualized by phosphorimaging. Authentic standards (C15–C120) were co-chromatographed and visualized by iodine vapor staining. For assays with SlCPT2 and SlCPT6 (the short-chain SlCPTs), reaction products were hydrolyzed by the more time-consuming method of alkaline phosphatase treatment rather than incubation with acid prior to TLC analysis, because acid hydrolysis of short-chain polyisoprenoids results in chemical rearrangements of some of the product (but the structures of longer chain isoprenoids are not affected). The preferred substrate for each enzyme was defined as the substrate that resulted in the highest specific activity under defined sub-saturating concentrations.

Yeast culture conditions, transformation and microsomal CPTase activity assays

The yeast strain YG932 (*rer2*Δ mutant) (*MATα rer2Δ::kanMX4 ade2–101 ura3–52 his3Δ200 lys2–801*) has been described previously (Schenk *et al.*, 2001), and was routinely cultured in yeast peptone dextrose media (YPD) at 23°C. The *SlCPT3* gene was transferred to pYEP352, as previously described (Rush *et al.*, 2010), and yeast transformation was performed as described by Gietz and Schiestl (2007). Transformants were selected on 0.67% yeast nitrogen base without amino acids, 50 mM sodium succinate, pH 5.5, 2% glucose and all necessary auxotrophic requirements, except uracil. Preparation of microsomal membranes for CPT activity assays was performed as described by Rush *et al.* (2010).

RNAi-mediated knockdown of *NDPS1* (*SlCPT1*)

A 204 bp fragment of *NDPS1* (corresponding to base pairs 19–223) was amplified by PCR and ligated in a sense/antisense orientation into pRNA69 (Foster *et al.*, 2002) between the *Xho*I/*Eco*RI and *Bam*HI/*Xba*I restriction sites, respectively. The hairpin cassette was released by *Spe*I/*Sac*I digestion and transferred to the pZP212 binary vector (Hajdukiewicz *et al.*, 1994) between the *Xba*I/*Sac*I restriction sites. For trichome-specific RNAi-mediated knockdown of *NDPS1*, the CaMV 35S promoter in pRNA69 was released by *Sac*I/*Xho*I digestion and replaced by the methyl ketone synthase 1 promoter (*MKS1*, Genbank accession number GU98105.1), which was obtained from *S. habrochaites* genomic DNA by PCR. The specificity of the *MKS1* promoter was confirmed by placing it upstream of GFP between the *Age*I and *Bam*HI sites of pSAT-EGFP–N1 (Tzfira *et al.*, 2005). The expression cassette was digested using PI-*Psp*I, and ligated into the corresponding sites of the pPZP-RCS2 binary vector (Tzfira *et al.*, 2005). The binary vectors were introduced into tomato by the University of Nebraska Plant Transformation Facility (http://biotech.unl.edu/plant-transformation). GFP fluorescence in transgenic tomato type VI trichomes was visualized using a Nikon Eclipse E600 Y–FL fluorescence microscope (http://www.nikon-instruments.jp) equipped with a 100 W mercury arc lamp, 505 nm dichroic mirror and using filter settings of 450–490 nm and 520–560 nm for GFP excitation and emission, respectively.

Terpene extraction and analysis

For analysis of total terpenes, approximately 200 mg of 3-week old leaf material was ground to a pulp in 2 ml hexane containing 34 μg ml^{-1} 1,2–dimethoxyphenol (internal standard) using a glass mortar and pestle, and vortexed vigorously for 1 min. The extract was filtered through glass wool, dried using anhydrous $MgSO_4$, and concentrated to a final volume of 0.2 ml. A 2 μl aliquot was injected into a QP–5000 GC–MS system (Shimadzu) (http://www.shimadzu.com/) equipped with an EC–WAX column (Grace Davison) (http://www.discoverysciences.com/) and analyzed as described by Falara *et al.* (2011). Terpenes were quantified by constructing standard concentration curves for β–phellandrene and β–caryophyllene.

ACCESSION NUMBERS

The GenBank accession numbers for the sequences referred to in this paper are given in parentheses: SlCPT1 (NM_001247704), SlCPT2 (JX943884), SlCPT3 (JX943885), SlCPT4 (JX943886), SlCPT5 (JX943887), SlCPT6 (JX943888) and SlCPT7 (JX943889).

ACKNOWLEDGEMENTS

We thank Thomas Clemente and the University of Nebraska plant transformation facility for generating transgenic tomato plants. We also thank Charles Waechter and Jeffrey Rush (University of Kentucky, Department of Molecular and Cellular Biochemistry, University of Kentucky College of Medicine, Lexington, Kentucky) for providing the yeast *rer2*Δ mutant and the *E. coli* UPPS construct, the members of the *Solanum* Trichome Project (http://www.trichome.msu.edu) for many fruitful discussions, and Greg Sobocinski (University of Michigan, Department of Molecular, Cellular and Developmental Biology, Ann Arbor, Michigan) for technical advice on confocal microscopy. This work was supported by

US National Science Foundation awards DBI-0604336 and IOS-1025636 and by the Agricultural and Food Research Initiative Competitive grant number 2008-35318-04541.

SUPPORTING INFORMATION

Additional Supporting Information may be found in the online version of this article.

Figure S1. Gene, cDNA and amino acid sequences of members of the tomato CPT family.

Figure S2. Names and accession numbers of all CPT sequences used for phylogenetic analysis in Figure 2.

Figure S3. GC–MS analysis of the product of *SlCPT6*.

Figure S4. GC–MS analysis of the product of *SlCPT2*.

Figure S5. Volatile terpene analysis of wild-type and NDPS RNAi lines.

Table S1. Synthetic oligonucleotides used in this study.

REFERENCES

Ambo, T., Noike, M., Kurokawa, H. and Koyama, T. (2008) Cloning and functional analysis of novel short-chain *cis*–prenyltransferases. *Biochem. Biophys. Res. Commun.* **375**, 536–540.

Asawatreratanakul, K., Zhang, Y.W., Wititsuwannakul, D., Wititsuwannakul, R., Takahashi, S., Rattanapittayaporn, A. and Koyama, T. (2003) Molecular cloning, expression and characterization of cDNA encoding *cis*–prenyltransferases from *Hevea brasiliensis*. A key factor participating in natural rubber biosynthesis. *Eur. J. Biochem.* **270**, 4671–4680.

Austin, J.R. II, Frost, E., Vidi, P.A., Kessler, F. and Staehelin, L.A. (2006) Plastoglobules are lipoprotein subcompartments of the chloroplast that are permanently coupled to thylakoid membranes and contain biosynthetic enzymes. *Plant Cell*, **18**, 1693–1703.

Bajda, A., Chojnacki, T., Hertel, J., Swiezewska, E., Wojcik, J., Kaczkowska, A., Marczewski, A., Bojarczuk, T., Karolewski, P. and Oleksyn, J. (2005) Light conditions alter accumulation of long chain polyprenols in leaves of trees and shrubs throughout the vegetation season. *Acta Biochim. Pol.* **52**, 233–241.

Bonk, M., Hoffmann, B., Von Lintig, J., Schledz, M., Al–Babili, S., Hobeika, E., Kleinig, H. and Beyer, P. (1997) Chloroplast import of four carotenoid biosynthetic enzymes *in vitro* reveals differential fates prior to membrane binding and oligomeric assembly. *Eur. J. Biochem.* **247**, 942–950.

Burke, C.C., Wildung, M.R. and Croteau, R. (1999) Geranyl diphosphate synthase: cloning, expression, and characterization of this prenyltransferase as a heterodimer. *Proc. Natl Acad. Sci. USA*, **96**, 13062–13067.

Cheniclet, C., Rafia, F., Saint-Guily, A., Verna, A. and Carde, J.P. (1992) Localization of the enzyme geranylgeranylpyrophosphate synthase in *Capsicum* fruits by immunogold cytochemistry after conventional chemical fixation or quick-freezing by freeze-substitution. Labelling evolution during fruit ripening. *Biol. Cell*, **75**, 145–154.

Chojnacki, T. and Vogtman, T. (1984) The occurrence and seasonal distribution of C50–C60 polyprenols and of C100 and similar long-chain polyprenols in leaves of plants. *Acta Biochim. Pol.* **31**, 115–126.

Ciepichal, E., Jemiola-Rzeminska, M., Hertel, J., Swiezewska, E. and Strzalka, K. (2011) Configuration of polyisoprenoids affects the permeability and thermotropic properties of phospholipid/polyisoprenoid model membranes. *Chem. Phys. Lipids* **164**, 300–306.

Cunillera, N., Arró, M., Forés, O., Manzano, D. and Ferrer, A. (2000) Characterization of dehydrodolichyl diphosphate synthase of *Arabidopsis thaliana*, a key enzyme in dolichol biosynthesis. *FEBS Lett.* **477**, 170–174.

van Der Hoeven, R.S., Monforte, A.J., Breeden, D., Tanksley, S.D. and Steffens, J.C. (2000) Genetic control and evolution of sesquiterpene biosynthesis in *Lycopersicon esculentum* and *L. hirsutum*. *Plant Cell*, **12**, 2283–2294.

Ducluzeau, A.L., Wamboldt, Y., Elowsky, C.G., Mackenzie, S.A., Schuurink, R.C. and Basset, G.J. (2012) Gene network reconstruction identifies the authentic *trans*–prenyl diphosphate synthase that makes the solanesyl moiety of ubiquinone–9 in Arabidopsis. *Plant J.* **69**, 366–375.

Eugeni-Piller, L., Besagni, C., Ksas, B., Rumeau, D., Bréhélin, C., Glauser, G., Kessler, F. and Havaux, M. (2011) Chloroplast lipid droplet type II NAD(P)H quinone oxidoreductase is essential for prenylquinone metabolism and vitamin K1 accumulation. *Proc. Natl Acad. Sci. USA*, **108**, 14354–14359.

Falara, V., Akhtar, T.A., Nguyen, T.T.H. *et al.* (2011) The tomato terpene synthase gene family. *Plant Physiol.* **157**, 770–789.

Foster, T.M., Lough, T.J., Emerson, S.J., Lee, R.H., Bowman, J.L., Forster, R. L. and Lucas, W.J. (2002) A surveillance system regulates selective entry of RNA into the shoot apex. *Plant Cell*, **14**, 1497–1508.

Fridman, E., Wang, J., Iijima, Y., Froehlich, J.E., Gang, D.R., Ohlrogge, J. and Pichersky, E. (2005) Metabolic, genomic, and biochemical analyses of glandular trichomes from the wild tomato species *Lycopersicon hirsutum* identify a key enzyme in the biosynthesis of methylketones. *Plant Cell*, **17**, 1252–1267.

Fujihashi, M., Zhang, Y.W., Higuchi, Y., Li, X.Y., Koyama, T. and Miki, K. (2001) Crystal structure of *cis*–prenyl chain elongating enzyme, undecaprenyl diphosphate synthase. *Proc. Natl Acad. Sci. USA*, **98**, 4337–4342.

Gietz, R.D. and Schiestl, R.H. (2007) Large-scale high-efficiency yeast transformation using the LiAc/SS carrier DNA/PEG method. *Nat. Protoc.* **2**, 38–41.

Hajdukiewicz, P., Svab, Z. and Maliga, P. (1994) The small, versatile pPZP family of *Agrobacterium* binary vectors for plant transformation. *Plant Mol. Biol.* **25**, 989–994.

Harrison, K.D., Park, E.J., Gao, N., Kuo, A., Rush, J.S., Waechter, C.J., Lehrman, M.A. and Sessa, W.C. (2011) Nogo–B receptor is necessary for cellular dolichol biosynthesis and protein *N*–glycosylation. *EMBO J.* **30**, 2490–2500.

Hirooka, Y., Bamba, T., Fukusaki, E. and Kobayashi, A. (2003) Cloning and kinetic characterization of *Arabidopsis thaliana* solanesyl diphosphate synthase. *Biochem. J.* **370**, 679–686.

Kera, K., Takahashi, S., Sutoh, T., Koyama, T. and Nakayama, T. (2012) Identification and characterization of a *cis*,*trans*–mixed heptaprenyl diphosphate synthase from *Arabidopsis thaliana*. *FEBS J.* **279**, 3813–3827.

Kharel, Y. and Koyama, T. (2003) Molecular analysis of *cis*–prenyl chain elongating enzymes. *Nat. Prod. Rep.* **20**, 111–118.

Kharel, Y., Takahashi, S., Yamashita, S. and Koyama, T. (2006) Manipulation of prenyl chain length determination mechanism of cis-prenyltransferases. *FEBS J.* **273**, 647–657.

Kirby, J. and Keasling, J.D. (2009) Biosynthesis of plant isoprenoids: perspectives for microbial engineering. *Annu. Rev. Plant Biol.* **60**, 335–355.

Lange, B.M. and Ghassemian, M. (2003) Genome organization in *Arabidopsis thaliana*: a survey for genes involved in isoprenoid and chlorophyll metabolism. *Plant Mol. Biol.* **51**, 925–948.

Liang, P.H., Ko, T.P. and Wang, A.H. (2002) Structure, mechanism, and function of prenyltransferases. *Eur. J. Biochem.* **269**, 3339–3354.

Liu, M.C., Wang, B.J., Huang, J.K. and Wang, C.S. (2011) Expression, localization and function of a *cis*–prenyltransferase in the tapetum and microspores of lily anthers. *Plant Cell Physiol.* **52**, 1487–1500.

McGarvey, D.J. and Croteau, R. (1995) Terpenoid metabolism. *Plant Cell* **7**, 1015–1026.

Nelson, B.K., Cai, X. and Nebenführ, A. (2007) A multicolored set of *in vivo* organelle markers for co-localization studies in Arabidopsis and other plants. *Plant J.* **51**, 1126–1136.

Oh, S.K., Han, K.H., Ryu, S.B. and Kang, H. (2000) Molecular cloning, expression, and functional analysis of a *cis*–prenyltransferase from *Arabidopsis thaliana*: implications in rubber biosynthesis. *J. Biol. Chem.* **275**, 18482–18488.

Phillips, M.A., D'Auria, J.C., Gershenzon, J. and Pichersky, E. (2008) The *Arabidopsis thaliana* type I isopentenyl diphosphate isomerases are targeted to multiple subcellular compartments and have overlapping functions in isoprenoid biosynthesis. *Plant Cell* **20**, 677–696.

Post, J., van Deenen, N., Fricke, J. *et al.* (2012) Laticifer-specific *cis*–prenyltransferase silencing affects the rubber, triterpene, and inulin content of *Taraxacum brevicorniculatum*. *Plant Physiol.* **158**, 1406–1417.

Rodríguez-Concepción, M. and Boronat, A. (2002) Elucidation of the methylerythritol phosphate pathway for isoprenoid biosynthesis in bacteria and plastids. A metabolic milestone achieved through genomics. *Plant Physiol.* **130**, 1079–1089.

Rush, J.S., Matveev, S., Guan, Z., Raetz, C.R.H. and Waechter, C.J. (2010) Expression of functional bacterial undecaprenyl pyrophosphate synthase in the yeast *rer2*Δ mutant and CHO cells. *Glycobiology*, **20**, 1585–1593.

Sakaihara, T., Honda, A., Tateyama, S. and Sagami, H. (2000) Subcellular fractionation of polyprenyl diphosphate synthase activities responsible for the syntheses of polyprenols and dolichols in spinach leaves. *J. Biochem.* **128**, 1073–1078.

Sallaud, C., Rontein, D., Onillon, S. *et al.* (2009) A novel pathway for sesquiterpene biosynthesis from *Z,Z*–farnesyl pyrophosphate in the wild tomato *Solanum habrochaites*. *Plant Cell* **21**, 301–317.

Sanmiya, K., Ueno, O., Matsuoka, M. and Yamamoto, N. (1999) Localization of farnesyl diphosphate synthase in chloroplasts. *Plant Cell Physiol.* **40**, 348–354.

Sato, M., Sato, K., Nishikawa, S., Hirata, A., Kato, J. and Nakano, A. (1999) The yeast *RER2* gene, identified by endoplasmic reticulum protein localization mutations, encodes *cis*–prenyltransferase, a key enzyme in dolichol synthesis. *Mol. Cell. Biol.* **19**, 471–483.

Schenk, B., Fernandez, F. and Waechter, C.J. (2001) The inside and outside of dolichyl phosphate biosynthesis and recycling in the endoplasmic reticulum. *Glycobiology* **11**, 61–70.

Schilmiller, A.L., Schauvinhold, I., Larson, M., Xu, R., Charbonneau, A.L., Schmidt, A., Wilkerson, C., Last, R.L. and Pichersky, E. (2009) Monoterpenes in the glandular trichomes of tomato are synthesized from a neryl diphosphate precursor rather than geranyl diphosphate. *Proc. Natl Acad. Sci. USA* **106**, 10865–10870.

Schilmiller, A.L., Miner, D.P., Larson, M., McDowell, E., Gang, D.R., Wilkerson, C. and Last, R.L. (2010) Studies of a biochemical factory: tomato trichome deep expressed sequence tag sequencing and proteomics. *Plant Physiol.* **153**, 1212–1223.

Schmidt, T., Lenders, M., Hillebrand, A., van Deenen, N., Munt, O., Reichelt, R., Eisenreich, W., Fischer, R., Prüfer, D. and Gronover, C.S. (2010) Characterization of rubber particles and rubber chain elongation in *Taraxacum koksaghyz*. *BMC Biochem.* **11**, 11.

Schulbach, M.C., Brennan, P.J. and Crick, D.C. (2000) Identification of a short (C15) chain *Z*–isoprenyl diphosphate synthase and a homologous long (C50) chain isoprenyl diphosphate synthase in *Mycobacterium tuberculosis*. *J. Biol. Chem.* **275**, 22876–22881.

Shridas, P., Rush, J.S. and Waechter, C.J. (2003) Identification and characterization of a cDNA encoding a long-chain *cis*–isoprenyltranferase involved in dolichyl monophosphate biosynthesis in the ER of brain cells. *Biochem. Biophys. Res. Commun.* **312**, 1349–1356.

Skorupinska-Tudek, K., Wojcik, J. and Swiezewska, E. (2008) Polyisoprenoid alcohols – recent results of structural studies. *Chem. Rec.* **8**, 33–45.

Spurgeon, S.L., Sathyamoorthy, N. and Porter, J.W. (1984) Isopentenyl pyrophosphate isomerase and prenyltransferase from tomato fruit plastids. *Arch. Biochem. Biophys.* **230**, 446–454.

Surmacz, L. and Swiezewska, E. (2011) Polyisoprenoids – secondary metabolites or physiologically important superlipids? *Biochem. Biophys. Res. Commun.* **407**, 627–632.

Swiezewska, E. and Danikiewicz, W. (2005) Polyisoprenoids: structure, biosynthesis and function. *Prog. Lipid Res.* **44**, 235–258.

Swiezewska, E., Sasak, W., Mańkowski, T., Jankowski, W., Vogtman, T., Krajewska, I., Hertel, J., Skoczylas, E. and Chojnacki, T. (1994) The search for plant polyprenols. *Acta Biochim. Pol.* **41**, 221–260.

Tamura, K., Dudley, J., Nei, M. and Kumar, S. (2007) MEGA4: Molecular Evolutionary Genetics Analysis (MEGA) software version 4.0. *Mol. Biol. Evol.* **24**, 1596–1599.

Tzfira, T., Tian, G.W., Lacroix, B., Vyas, S., Li, J., Leitner-Dagan, Y., Krichevsky, A., Taylor, T., Vainstein, A. and Citovsky, V. (2005) pSAT vectors: a modular series of plasmids for autofluorescent protein tagging and expression of multiple genes in plants. *Plant Mol. Biol.* **57**, 503–516.

Vigo, C., Grossman, S.H. and Drost-Hansen, W. (1984) Interaction of dolichol and dolichyl phosphate with phospholipid bilayers. *Biochim. Biophys. Acta* **774**, 221–226.

Vincent, F., Molin, D.D., Weiner, R.M., Bourne, Y. and Henrissat, B. (2010) Structure of a polyisoprenoid binding domain from *Saccharophagus degradans* implicated in plant cell wall breakdown. *FEBS Lett.* **584**, 1577–1584.

Wu, F.H., Shen, S.C., Lee, L.Y., Lee, S.H., Chan, M.T. and Lin, C.S. (2009) Tape–*Arabidopsis* sandwich – a simpler Arabidopsis protoplast isolation method. *Plant Methods*, **5**, 16.

Ytterberg, A.J., Peltier, J.B. and van Wijk, K.J. (2006) Protein profiling of plastoglobules in chloroplasts and chromoplasts. A surprising site for differential accumulation of metabolic enzymes. *Plant Physiol.* **140**, 984–997.

Yu, L., Peña-Castillo, L., Mnaimneh, S., Hughes, T.R. and Brown, G.W. (2006) A survey of essential gene function in the yeast cell division cycle. *Mol. Biol. Cell* **11**, 4736–4747.

Yu, G., Nguyen, T.T., Guo, Y., Schauvinhold, I., Auldridge, M.E., Bhuiyan, N., Ben-Israel, I., Iijima, Y., Fridman, E., Noel, J.P. and Pichersky, E. (2010) Enzymatic functions of wild tomato methylketone synthases 1 and 2. *Plant Physiol.* **154**, 67–77.

Zhang, H., Ohyama, K., Boudet, J., Chen, Z., Yang, J., Zhang, M., Muranaka, T., Maurel, C., Zhu, J.K. and Gong, Z. (2008) Dolichol biosynthesis and its effects on the unfolded protein response and abiotic stress resistance in *Arabidopsis*. *Plant Cell*, **20**, 1879–1898.

Zhou, G.P. and Troy, F.A. II (2003) Characterization by NMR and molecular modeling of the binding of polyisoprenols and polyisoprenyl recognition sequence peptides: 3D structure of the complexes reveals sites of specific interactions. *Glycobiology*, **13**, 51–71.